Protein Science (1999), *8*:958–968. Cambridge University Press. Printed in the USA.

Energetic analysis of an antigen/antibody interface: Alanine scanning mutagenesis and double mutant cycles on the HyHEL-10/lysozyme interaction

JAUME PONS, ARVIND RAJPAL,[1] AND JACK F. KIRSCH

Departments of Chemistry and Molecular and Cell Biology, University of California, and Center for Advanced Materials, Lawrence Berkeley National Laboratory, Berkeley, California 94720

(RECEIVED October 14, 1998; ACCEPTED December 23, 1998)

Abstract

Alanine scanning mutagenesis of the HyHEL-10 paratope of the HyHEL-10/HEWL complex demonstrates that the energetically important side chains (hot spots) of both partners are in contact. A plot of $\Delta\Delta G_{\text{HyHEL-10\_mutant}}$ vs. $\Delta\Delta G_{\text{HEWL\_mutant}}$ for the five of six interacting side-chain hydrogen bonds is linear (Slope = 1). Only 3 of the 13 residues in the HEWL epitope contribute >4 kcal/mol to the free energy of formation of the complex when replaced by alanine, but 6 of the 12 HyHEL-10 paratope amino acids do. Double mutant cycle analysis of the single crystallographically identified salt bridge, $D32_H/K97$, shows that there is a significant energetic penalty when either partner is replaced with a neutral side-chain amino acid, but the $D32_HN/K97M$ complex is as stable as the WT. The role of the disproportionately high number of Tyr residues in the CDR was evaluated by comparing the $\Delta\Delta G$ values of the Tyr → Phe vs. the corresponding Tyr → Ala mutations. The nonpolar contacts in the *light* chain contribute only about one-half of the total $\Delta\Delta G$ observed for the Tyr → Ala mutation, while they are significantly more important in the *heavy* chain. Replacement of the $N31_L/K96$ hydrogen bond with a salt bridge, $N31D_L/K96$, destabilizes the complex by 1.4 kcal/mol. The free energy of interaction, $\Delta\Delta G_{int}$, obtained from double mutant cycle analysis showed that $\Delta\Delta G_{int}$ for any complex for which the HEWL residue probed is a major immunodeterminant is very close to the loss of free energy observed for the HyHEL-10 single mutant. Error propagation analysis of double mutant cycles shows that data of atypically high precision are required to use this method meaningfully, except where large $\Delta\Delta G$ values are analyzed.

Keywords: alanine scan mutagenesis; antibody; antigen; double mutant cycles; epitope mapping; hen egg-white lysozyme; monoclonal antibody HyHEL-10; protein–protein interaction

Crystallographically defined two-protein complexes are especially useful as starting points to evaluate the quantitative details of protein–protein interaction. Several specific additional advantages are provided by antibody/protein antigen complexes because the vast antibody recognition repertoire is isolated to the small CDR region while the remainder of the antibody is largely invariant. The interfaces of antibody/protein antigen complexes are characterized by 650–1,000 Å^2 of buried surface area, 12–20 contact residues from each partner, 8–13 hydrogen bonds, and an occasional salt bridge (Janin & Chothia, 1990). These complexes also show an intermediate degree of shape complementarity at the interface (that is less than that of protease–protease inhibitor complexes, but greater than that of a T cell receptor with a major histocompatibility complex complex (Ysern et al., 1998)). The complex formed from hen egg-white lysozyme (HEWL) and the monoclonal antibody HyHEL-10 has been extensively studied in this (Kam-Morgan et al., 1993; Rajpal et al., 1998; Taylor et al., 1998) and other laboratories (i.e., Smith-Gill et al., 1984; Padlan et al., 1989; Xavier & Willson, 1998).

Fourteen hydrogen bonds, 111 van der Waals contacts, and one salt bridge have been crystallographically identified in the interface of the complex Fab-10/HEWL (Padlan et al., 1989). Kam-Morgan et al. (1993) showed that replacement of Arg21 with any of eight other amino acids destabilizes the complex by ~2.2 kcal/mol. The value of $\Delta\Delta G$ effected by mutagenesis of Asp101 is

Reprint requests to: Jack F. Kirsch, Department of Molecular and Cell Biology, 229 Stanley Hall, University of California, Berkeley, California 94720; e-mail: jfkirsch@uclink4.berkeley.edu.

[1]Present address: Molecular Sciences Department, Pfizer Inc., Eastern Point Road, Groton, Connecticut 06340.

Abbreviations: HEWL, hen (chicken) egg-white lysozyme; HyHEL-10, monoclonal antibody raised against HEWL; CDR, complementary determining region; Fab-10, antigen binding fragment of HyHEL-10 antibody; scFv-10, single-chain variable fragment of HyHEL-10 antibody; subscripts L and H, antibody light and heavy chain, respectively; $\Delta\Delta G_D$, change in free energy (WT-mutant); WT, wild-type; K_D, dissociation constant for the scFv-10/HEWL complex; k_{on} and k_{off}, association and dissociation rate constants for the scFv-10/HEWL complex.

dependent, however, on the side-chain volume of the replacement amino acid. For example, the D101G and D101F complexes have $\Delta\Delta G$ values of 0.2 and 2.2 kcal/mol, respectively compared to WT.

Rajpal et al. (1998) found that the major HEWL immunodeterminants as defined by alanine scanning mutagenesis are Tyr20, Lys96, and Lys97 with $\Delta\Delta G$ values of 4.3, 6.5, and 5.6 kcal/mol, respectively. Combinations of alanine mutations in the HEWL epitope showed that the minor immunodeterminants buttress the major ones, thereby stabilizing the reactive conformation of the antigen (Rajpal & Kirsch, 1999). The kinetics of interaction of HyHEL-10 with WT and mutant HEWL proved important in developing an experimental strategy for delineating protein docking trajectories (Taylor et al., 1998).

Previous studies on the contribution of the HyHEL-10 paratope residues have focused on the mutational analysis of the single salt bridge (Tsumoto et al., 1996) and the heavy chain Tyr residues (Tsumoto et al., 1995) (see Results and discussion). Xavier and Willson (1998) recently compared the kinetics of HEWL association with HyHEL-10 with those of the nonoverlapping monoclonal antibody HyHEL-5.

Although the HEWL epitope has been extensively probed, the general energetic topology of the HyHEL-10 paratope needs further analysis. The free energy changes in complex formation resulting from paratope mutation that are complementary to those already available from the epitope would allow double mutant cycle analysis (Schreiber & Fersht, 1995).

We report here the thermodynamic and kinetic results of alanine scanning mutagenesis of the HyHEL-10 paratope. Tyrosine residues were additionally replaced with Phe to dissect the effect of the hydroxyl group from that of the aromatic ring. Single and double mutant cycle analysis allows the evaluation of the energetic contributions of all of the putative hydrogen bond and salt bridge interactions. A salt bridge was introduced to replace the $N31_L$/K96 hydrogen bond interaction to test a theoretical prediction that this combination would increase the stability of the complex by 5.6 kcal/mol (Pomès et al., 1995).

Results and discussion

Mutant selection rationale

The complete data set of all determined rate and equilibrium constants, their associated standard errors, and calculated $\Delta\Delta G$ values are provided in the Appendix.

Eighteen of the CDR residues of HyHEL-10 interact with HEWL (Table 1). The complexes containing alanine mutants of those amino acids whose side chains interact with HEWL, indicated by underscoring in Table 1, were investigated to explore individual contributions to overall stability. The tyrosines were also converted to phenylalanine to isolate the effects of the phenolic hydroxyl groups from the ring interactions. Additionally, the mutations $D32_HN$, $N31_L$ (D,E), and $W95_HF$ were introduced to evaluate the $D32_H$/K97 salt bridge, the $N31_L$/K96 hydrogen bond, and the effect of a more conservative substitution for tryptophan, respectively.

The paratope residues $G30_L$ and $N92_L$ were not mutated because these amino acids make only main-chain contacts in the complex. A single framework residue, $T30_H$, makes contact with HEWL. However, the $T30_H$A mutation does not affect the stability of the complex (data not shown).

Table 1. *Crystallographically identified contacts in the HyHEL-10/Lysozyme (HEWL) interface*[a]

HyHEL-10	HEWL	HyHEL-10	HEWL
V_L		V_H	
G30	G16	T30[c]	R73(h)
N31	H15, G16, **K96**(h)[b]	S31	R73(h), L75
N32	G16(h), **Y20**	D32	**K97**(s)
Y50	N93, **K96**	Y33	W63, **K97**(h), I98, S100, D101
Q53	T89, N93(h)		
S91	**Y20** (h)	Y50	R21(h), S100(h)
N92	**Y20**, R21(h)	S52	D101
Y96	R21 (h)	Y53	W63, L75, D101(h)
		S54	D101
		S56	D101, G102
		Y58	R21, S100, G102(h)
		W95	R21, **K97**, S100

[a] Padlan et al. (1989). The numbering is that of Kabat et al. (1991).
[b] Codes: h, hydrogen bond (see Table 2 for donor/acceptor identification.); s, salt bridge. The HEWL residues highlighted in bold have been identified as major contributors to the free energy of complex formation by alanine scanning mutagenesis (Rajpal et al., 1998). The contributions of the underlined HyHEL-10 side-chain residues were evaluated in this work.
[c] Framework residue.

Alanine mutants: Paratope topology

The changes in $\Delta\Delta G$ values for the stabilities of the HyHEL-10/HEWL complexes effected by alanine and phenylalanine substitutions in the paratope are shown in Figure 1 (top right), together with the corresponding effects for alanine replacements in the epitope (Fig. 1, bottom right). The color coding is defined in the legend.

As a rule, the antibody hot, warm, and null spot residues interact with the correspondingly important HEWL amino acids. $D32_H$ and $Y50_H$ are, respectively, warm and hot spot exceptions that are discussed below. Previous investigations of protein–protein interaction report similar correspondence of the importance of complementary residues (Clackson & Wells, 1995; Goldman et al., 1997). Such complementarity should be expected; i.e., if residue *X* makes a strong interaction only with *Y* as signaled by the large $\Delta\Delta G$ associated with an $X \rightarrow$ Ala substitution, then that specific relationship would be sharply reduced or eliminated by alteration of *either* partner. The lack of such correspondence is in fact an indication of additional interaction affecting at least one of the partners (see below).

It is notable that 6 of the 12 HyHEL-10 residues in the paratope qualify as hot spots as defined in Figure 1, but only 3 of the 13 epitope residues fall into this category. The six HyHEL-10 hot spot side chains all contact the three dominant lysozyme hot spots. This difference in number of important affinity residues shows that stabilization of the complex is achieved by the accumulation of many productive cooperative interactions of the CDR residues with the fewer HEWL hot spots. Differences in the number of important residues between the two interfaces of a reacting pair of proteins have recently been reported for the interaction between human growth hormone and its receptor (Clackson et al., 1998). These authors suggest that quantitatively important side chains placed in loops will show more cooperativity than will those located in rigid structures, such as α-helices. The HyHEL-10/

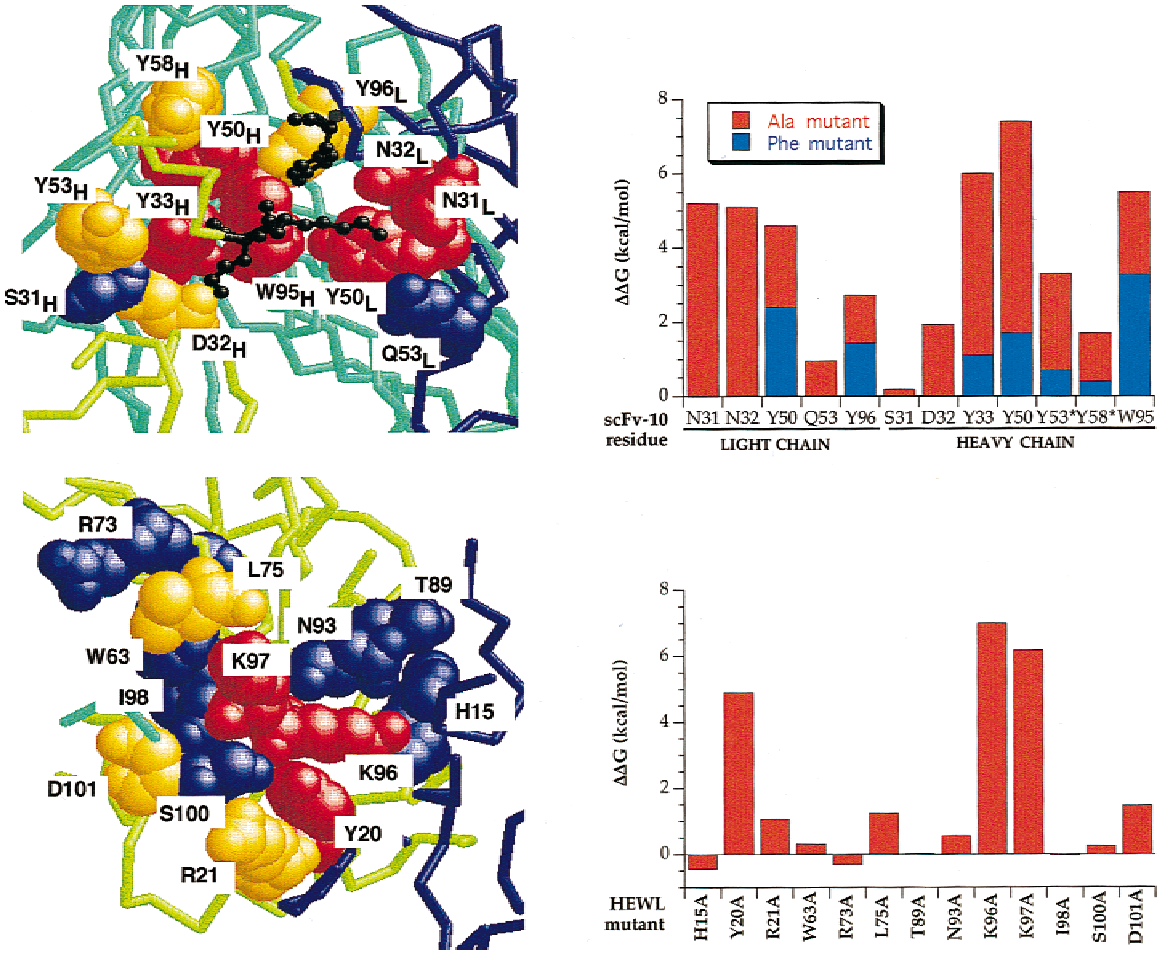

Fig. 1. A: CPK representation of HyHEL-10 paratope residues in contact with HEWL (top) and of the complementary HEWL epitope residues (bottom). Amino acids whose mutation to alanine gives a $\Delta\Delta G > 4$ kcal/mol (hot spots) are shown in red, those yielding 1 kcal/mol $< \Delta\Delta G <$ 4 kcal/mol (warm spots) are in yellow and those with $<$1 kcal/mol are in blue (null spots). Correct apposition of the structures can be visualized by folding the page horizontally. To aid in the positioning, the three major immunodeterminants of HEWL (Rajpal et al., 1998) are superimposed in black ball and stick models on the paratope structure (top). **B:** Histograms reporting the specific destabilization free energies for the mutations shown on the left: upper, paratope mutants. The total bar height reflects the Tyr → Ala mutations while the values in blue show the uniformly smaller effects of Tyr → Phe mutations in the paratope (HyHEL-10). Lower: destabilization of the HyHEL-10/HEWL complex by alanine scanning mutagenesis of the epitope. The values obtained here with the scFv of HyHEL-10/HEWL complexes are within ±0.5 kcal/mol of those previously reported for the corresponding Fab-10/HEWL complexes (Rajpal et al., 1998). Literature values for the $Y53_H$ (A,F), $Y58_H$(A,F), $Y33_H$F, and $Y50_H$F/HEWL (WT) complexes (*) are shown (Tsumoto et al., 1995).

HEWL interaction can be described similarly as two of the three hot spots contributed by HEWL are in an α-helix (Rajpal et al., 1998), while those from the antibody are distributed in the CDR loops.

The topology of the interaction shows that the hot spots are centrally located, but there is no clustering of hydrophobic hot spots in the core surrounded by hydrophilic residues in the periphery. Two of the three hot spots in the epitope have charged side chains, and 3 of the 10 important residues in the paratope are hydrophilic, 1 is hydrophobic, and 6 are tyrosines. Goldman et al. (1997) have noted that there appear to be two topological classes of protein–protein interaction. The first consists of a hydrophobic core surrounded by hydrophilic amino acids, and is exemplified by protein hormone/receptor complexes (Wells, 1996). The second is found in reactions of antibodies with protein antigens where hydrophobic and hydrophilic residues are not clustered (Dall'Acqua et al., 1996). A recently defined additional grouping is seen in the interaction between a T cell receptor with a nonapeptide/MHC complex, where an estimated 37% of the free energy of association was attributed to interactions with the centroid peptide while the remainder results from peripheral interactions of MGC with the T cell receptor (Manning et al., 1998).

Role of salt bridges

The ϵ-amino group of HEWL K97 forms a salt bridge with the side-chain carboxylate of $D32_H$ in the crystallographic structure of HEWL with Fab-10 (Padlan et al., 1989). These authors also noted a highly polar H-bond between the ϵ-amino group of HEWL K96 and Oδ1 of $N31_L$. Computational studies by Pomès et al. (1995) suggested that this H-bond might be converted to a salt bridge by

placing a negatively charged residue at position $N31_L$, resulting in a calculated 5.6 kcal/mol increase in the stability of the complex.

To study the contributions of the above-described interactions to the stability of this complex, the previously prepared HEWL mutants K97A, K97M, and K96A (Taylor et al., 1998) were employed together with the HyHEL-10 mutants $D32_HA$, $D32_HN$, $N31_LA$, $N31_LD$, and $N31_LE$. A double mutant cycle approach was applied to each interaction.

The double mutant cycle describing the effect of Ala replacements of HEWL K97 and of HyHEL-10 $D32_H$ on the thermodynamics of complex formation (Scheme 1, bottom) shows that there is a 1.6 kcal/mol *gain* in the stability of the complex when the second mutation is added to the deleterious HyHEL-10(WT)/HEWL (K97A) single mutant complex. Thus, these results indicate that the role of the negative charge of the HyHEL-10 $D32_H$ is only to neutralize the uncompensated positive charge of HEWL K97. This conclusion is supported by the observation that the value for the $D32_HA$/K97M complex is also 1.1 kcal/mol less stable than that of the WT (Appendix). Thus, burying the negative charge of $D32_H$ by neutralization of the Lys97 (HEWL) is inconsequential. Further support for this hypothesis was obtained by constructing a pair of mutants designed to maintain approximately the same steric bulk of the original ion pair, but which contribute only van der Waals interactions. The stability of the $D32_HN$/K97M complex is experimentally indistinguishable from that of the WT (Scheme 1, top). Thus, the salt bridge per se is thermodynamically insignificant. This set of substitutions emphasizes the need to extend replacement sets beyond simple alanine substitutions (see Rajpal et al., 1998, for additional examples), i.e., the results of the alanine scanning substitutions ($D32_HA$ with or without K97A) imply that the sale bridge contributes $\geq$1.9 kcal/mol while the mass conservative mutations $D32_HN$/K97M yield a much smaller figure (0.3 kcal/mol).

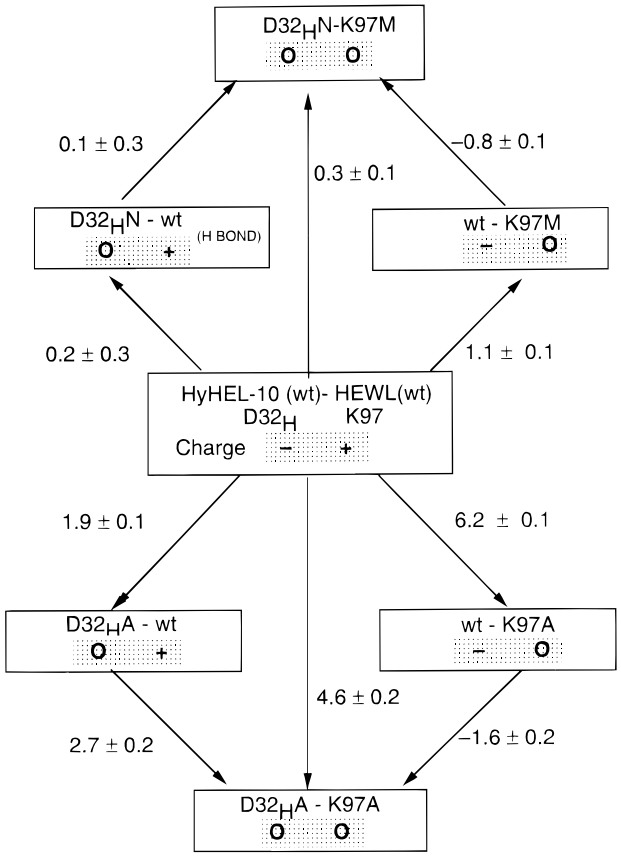

Scheme 1. Conservative (upper) and alanine (lower) replacement double mutant cycle analysis of the putative HyHEL-10 ($Asp32_H$)–HEWL (Lys97) salt bridge. Left: replacements of HyHEL-10 ($Asp32_H$) to Asn (upper) and Ala (lower); right: replacements of HEWL (Lys97) by Met (upper) and Ala (lower). The numerical values are in kcal/mol and give the $\Delta\Delta G$ with respect to the WT complex (shown at the center of the figure) that are obtained for the indicated mutations. Local charges are shown as (−) negative, (+) positive, and (○) neutral next to each complex.

The effects of the $D32_HA$, $D32_HN$, and $D32_HE$ mutations on the free energy of the corresponding WT HEWL complexes were evaluated calorimetrically by Tsumoto et al. (1996). The values of the $\Delta\Delta G$ of destabilization with respect to the WT complexes are close to those reported here. These mutations yield decreases in entropy of complex formation that are partially compensated by enthalpy decreases. The $D32_HN$ mutant showed the highest decrease in enthalpy, probably due to formation of a H-bond, but this mutation has a negligible effect on the stability of the complex. The decreased entropy of complex formation was interpreted in terms of an effect of a larger structural change when binding the mutant antibodies. Tsumoto et al., proposed that the salt bridge suppresses excess local conformational change upon association. The present work shows that the same result in terms of free energy is obtained by mutations that anchor the protein exclusively through interactions of uncharged residues.

The role of the HEWL K96/HyHEL-10 $N31_L$ hydrogen bond was evaluated by the double mutant cycle of Scheme 2, bottom. In double mutant cycles, the changes in free energy in the double mutant complex for a pair of residues ($\Delta\Delta G_{AB\rightarrow A'B'}$) is subtracted from the sum of the two single mutations to calculate the coupling energy ($\Delta\Delta G_{int}$) between those amino acids (Equation 1):

$$\Delta\Delta G_{int} = \Delta\Delta G_{A\rightarrow A'} + \Delta\Delta G_{B\rightarrow B'} - \Delta\Delta G_{AB\rightarrow A'B'}. \qquad (1)$$

K96 and $N31_L$ interact only through this hydrogen bond; therefore evaluation of the $\Delta\Delta G_{int}$ in this case allows the calculation of the contribution of this hydrogen bond to the free energy of formation of the complex as 4.7 kcal/mol (Table 2). This value is close to that obtained for the single $N31_LA$ mutation in HyHEL-10 (5.2 kcal/mol); therefore, the contribution of this H-bond is isolated and it is worth ~5 kcal/mol.

The proposal of Pomès et al. (1995) that replacement of $N31_L$ with aspartic acid to create a salt bridge and thus stabilize the complex by a calculated 5.6 kcal/mol was tested here via the $N31_LD$ and $N31_LE$ constructs. The calculated result was not verified experimentally; rather these mutant complexes are 1.4 kcal/mol ($N31_LD$) and 5.7 kcal/mol ($N31_LE$) less stable than those formed with WT HyHEL-10 (Scheme 2, top).

The two examples discussed above demonstrate that a charged residue in the epitope can be stabilized equally or better by a neutral H-bond donor/acceptor than by a counter ion. Hendsch and Tidor (1994) have pointed out that, in the majority of cases, the expected stabilization of salt bridges is compromised by large unfavorable desolvation contributions, and Mian et al. (1991) have argued that oriented dipoles are usually preferred over counter charges in stabilizing buried ionized groups. The burying of an uncompensated charge is highly unfavorable. This fact may be

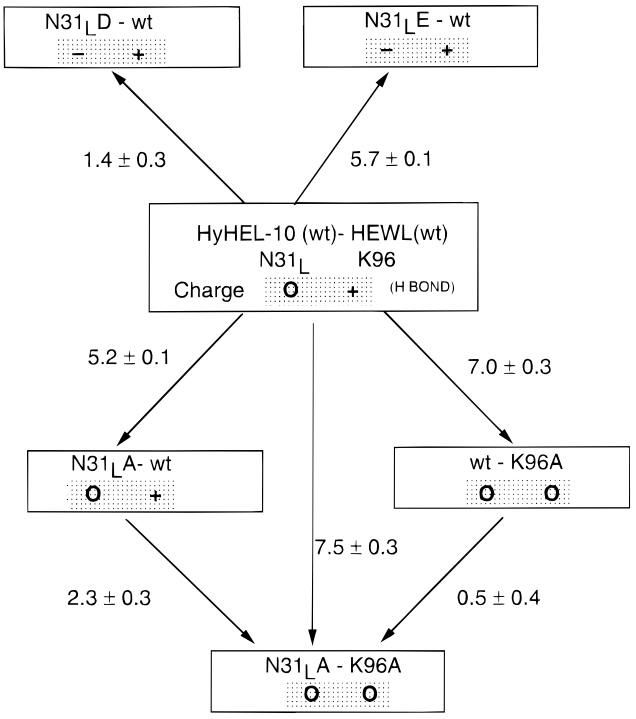

Scheme 2. Dissection of the free energy contribution of the $N31_L$-K96 hydrogen bond to the stability of the HyHEL-10/HEWL complex. Upper: Replacement of the neutral/positive hydrogen bond with a putative salt bridge by $N31_L$D and $N31_L$E mutations. Lower: Alanine replacement double mutant cycle. The numerical values are in kcal/mol and give the $\Delta\Delta G$ with respect to the WT complex (shown at the center of the figure) that are obtained for the indicated mutations. Local charges are shown as (−) negative, (+) positive, and (○) neutral next to each complex.

generally useful in dictating the specificity of antigen/antibody interactions, because antibodies that fail to compensate for charged residues will not bind well to the antigenic protein even with otherwise excellent surface complementarity. A particularly poignant demonstration of the role of salt bridges in specificity is found in the interaction between human growth hormone and its receptor, where the removal of a salt bridge by mutation of the receptor Arg43 to Leu destabilizes the complex by only 0.5 kcal/mol (Clackson et al., 1998), but this mutant receptor cross-reacts with bovine growth hormone, whereas the WT receptor does not (Souza et al., 1995; Goodman et al., 1996).

Role of hydrogen bonds

The energetic contributions to the free energy of formation of the complex of 13 of the 14 H-bonds proposed from the crystallographic structure are shown in Table 3. It is not possible to probe the main-chain/main-chain H-bond between $N92_L$ and HEWL R21 by site-directed mutagenesis. The role of the important H-bond K96/$N31_L$ was discussed above.

The values of $\Delta\Delta G$ obtained by amino acid replacements on HyHEL-10 correspond well with those obtained by mutation of the directly interacting residues on HEWL (Fig. 2). The strong correlation between $\Delta\Delta G$ occasioned by mutation of either partner argues that single mutations (Y to F, and others to Ala) do not generally overestimate hydrogen bond contributions. Most of the significant H-bonds in the interface contribute between 1–2 kcal/mol to the free energy of stabilization, as expected (Fersht et al., 1985; Alber et al., 1987; Serrano et al., 1992; Goldman et al., 1997). The proposed HyHEL-10 $S31_H$/HEWL R73, $Y58_H$/G102, S91/Y20, and T30/R73 H-bonds do not contribute significantly.

One neutral-neutral H-bond stands out for its high contribution to the stability of the complex: the HyHEL-10 $N32_L$ Nδ2 with G16 O (5.1 kcal/mol, $r = 3.24$ Å). The Nδ2 atom of $N32_L$ also appears to contact Cϵ1 and Cδ1 of Y20, and Cϵ of K96, in the crystallographic structure. Tyr20 and K96 are HEWL hot spots, and the later contacts are thus eliminated in the mutant $N32_L$A. This observation suggests that the value of 5.1 kcal/mol is an overestimate of the contribution of this H-bond. We tried to determine the energetic value for the interaction between $N32_L$ and Y20 by double mutant cycles, but no association with HEWL was observed in the double mutant, $N32_L$A/Y20A at [scFv] = 4 μM; therefore, the K_D is >8 μM. This H-bond cannot be examined by double mutant cycles as the backbone oxygen of G16 cannot be eliminated by site-directed mutagenesis. A possible explanation for this result would be that the $N32_L$A mutation elicits a conformational change in the antibody. This is, however, unlikely because the residue in position 32 is not a conformational determinant for the 2/11A class of CDR-L1 (Chothia et al., 1989; Martin & Thornton, 1996), to which the corresponding CDR of HyHEL-10 belongs.

Quantitative dissection of the free energy contribution of each of the paratope tyrosine residues

Davies and Cohen (1996) and Kabat et al. (1977) have noted the disproportionate number of tyrosine residues in CDRs, and Mian et al. (1991) have pointed out that there is a higher percentage in the heavy chain. It has been proposed that the explanation for the overabundance of tyrosine in CDRs is that the hydroxyphenyl side chain allows participation in both polar and apolar interactions. This is quantitatively significant for HyHEL-10, as 6 of the 10 important paratope residues are tyrosines ($\Delta\Delta G$ Tyr → Ala > 2.7 kcal/mol). Factoring the van der Waals interactions from the H-bonding contributions was accomplished by comparing the $\Delta\Delta G$ value of the Tyr → Phe vs. the corresponding Tyr → Ala mutation. The former isolates the H-bond value as nearly as can be done by site-directed mutagenesis, while the latter measures the sum of hydroxyl and ring contributions. The results given in Figure 1 show that the $\Delta\Delta G$ associated with each Tyr → Ala is invariably greater than that of the corresponding Tyr → Phe mutation. The relative contributions vary however. It is notable that the nonpolar contacts in the *light* chain contribute only about one-half of the total $\Delta\Delta G$ observed for the Tyr → Ala mutation, while they are significantly more important in the *heavy* chain. This difference is highlighted by the plot of Figure 3, where separate linear correlations are observed for plots of $\Delta\Delta G$(Tyr → Phe) vs. $\Delta\Delta G$(Tyr → Ala) for the light and heavy chains. Any conclusion drawn from the relation of Figure 3 must be tempered by the limitation that there are only two tyrosines in the light chain. Nonetheless, the difference for each of the two light chain tyrosines is clearly outside the range of the much better defined heavy chain correlation.

The slope for the light chain tyrosine mutations is 0.5 while that for the heavy chain residues is 0.2, emphasizing the relative dominance of nonpolar interactions in the heavy chain. Consistent with this set of observations is the fact that nonpolar residues dominate the important ($\Delta\Delta G_{(X\rightarrow Ala)} > 1$ kcal/mol) heavy chain contributions to the HyHEL-10 paratope (Fig. 1; Tyr4, Trp1, and Asp1)

Table 2. *Double mutant cycle analysis of the coupling energies between the indicated mutant pairs in the HyHEL-10/HEWL complex for adjacent partners*[a]

HyHEL-10 mutants	$\Delta\Delta G$[b] (kcal/mol) HyHEL-10 mutants	HEWL mutants	$\Delta\Delta G$[b] (kcal/mol) HEWL mutants	Double mutant $\Delta\Delta G$[b] (kcal/mol)	Lost interaction[a]	$\Delta\Delta G_{int}$[c] (kcal/mol)
V_L						
$N31_LA$	5.2 ± 0.1	K96A	7.0 ± 0.3	7.5 ± 0.3	H bond	4.7 ± 0.4
$Y50_LA$	4.6 ± 0.1	K96A	7.0 ± 0.3	7.8 ± 1.0	vdW[d]	3.8 ± 1.1
$Y96_LA$	2.7 ± 0.1	R21A	1.1 ± 0.1	5.7 ± 0.3	H bond	−1.9 ± 0.3
V_H						
$D32_HA$	1.9 ± 0.1	K97A	6.2 ± 0.1	4.6 ± 0.2	Salt bridge	3.5 ± 0.2
$Y33_HA$	6.0 ± 0.1	K97A	6.2 ± 0.1	7.2 ± 0.2	vdW + main-chain H bond	5.0 ± 0.2
$Y50_HA$	7.4 ± 0.4	R21A	1.1 ± 0.1	8.0 ± 0.7	H bond	0.5 ± 0.8
$W95_HA$	5.5 ± 0.2	K97A	6.2 ± 0.1	NB[e]	vdW	NA[f]

[a] Structural data from Padlan et al. (1989).

[b] The $\Delta\Delta G$ values are defined as $\Delta\Delta G = RT \ln(K_{mut\_complex}/K_{WT\_complex})$, where K is the dissociation constant.

[c] Coupling energies are defined as $\Delta\Delta G_{int} = \Delta\Delta G_{A-A'}$ (column 2) + $\Delta\Delta G_{B-B'}$ (column 4) − $\Delta\Delta G_{AB-A'B'}$ (column 5); A and B refer to residues present in WT HyHEL-10 and HEWL, respectively, A′ and B′ represent residues present in mutant HyHEL-10 and HEWL, respectively.

[d] vdW = van der Waal.

[e] NB, no binding at 20 μM HyHEL-10: K_D >40 μM, $\Delta\Delta G$ >8.5 kcal/mol.

[f] Not available, see footnote e.

while the converse obtains for the light chain (Tyr2, Asn2). Thus, at least for the HyHEL-10/HEWL interaction, it can be concluded that the molecular "cement" is composed of rather clearly divided nonpolar heavy chain and polar light chain contributions.

Interestingly the magnitudes of energetic contributions of the dominant tyrosines of the light chain ($Y50_L$) and heavy chain ($Y50_H$) cannot be rationalized readily from the structure of the complex. The large effect of the $Y50_LF$ mutation (2.4 kcal/mol) leads to the expectation of the most significant H-bond; however the closest atoms to this hydroxyl group are Cβ and Cδ of HEWL K96, at 3.57 and 3.72 Å, respectively, and the closest heteroatom, the main-chain O of HEWL N93, is too distant to make a H-bond (4.03 Å). Thus, the explanation for the importance of this Tyr hydroxyl group is not apparent. $Y50_H$ shows the highest contribution for a paratope residue ($\Delta\Delta G$ Tyr → Ala 7.4 kcal/mol), and it is the only antibody hot spot that is not in direct contact with an epitope hot spot. However, it does contact with the HEWL warm spot, R21. $Y50_H$ also makes multiple contacts with the important paratope side chains ($W95_H$, $Y96_L$, $Y58_H$), suggesting that the large contribution identified by the $Y50_HA$ mutation is the result of a structural perturbation of the paratope binding site. Rajpal and Kirsch (1999) noted that warm spot mutations affect the value of adjacent hot spots in the HEWL epitope, and suggested that the warm spot residues function as buttresses of the hot spot contributors. The preceding discussion excludes the possible role of intervening water molecules in H-bond complexes, as their positions are not apparent in a 3 Å structure.

The role of the heavy chain tyrosines was previously studied by Tsumoto et al. (1995) who converted $Y33_H$, $Y50_H$, $Y53_H$, and $Y58_H$ to Ala, Leu, and Trp. The enthalpic and entropic contributions for those mutants that could be obtained in sufficient quantity were evaluated calorimetrically. The $Y33_HA$ and $Y50_HA$ constructs could not be purified by HEWL affinity chromatography, and it was proposed that $Y33_H$ and $Y50_H$ are major contributors to the free energy of complex formation. This suggestion is supported by the present results.

The Tyr → Phe and Tyr → Ala mutations taken singly and together define the quantitative importance of the CDR tyrosines of HyHEL-10 in the formation of the HyHEL-10/HEWL complex. Padlan (1990) discussed the advantages of aromatic over aliphatic side-chain amino acids in the CDRs. He pointed out that the fusion of many atoms in a ring system immobilizes that side chain in the free antibody, while aliphatic side chains generally have more conformational entropy in the free antibody, which would have to be frozen out in the complex.

Double mutant cycles

Carter et al. (1984) introduced double mutant cycle analysis to study structural changes in the active site of a tyrosyl-tRNA synthetase. Subsequent applications include those of Serrano et al. (1990, 1992) in barnase and Pons et al. (1995) in a β-glucanase. These investigations are applications of double mutant cycles on two amino acids within the same molecule, but the technique has been recently extended to the investigation of protein–protein interactions (barnase/barstar, Schreiber & Fersht, 1995; Frisch et al., 1997; Schreiber et al., 1997; and D1.3/E5.2, Goldman et al., 1997; and D1.3/HEWL, Dall'Acqua et al., 1998). As described above (see Role of salt bridges), double mutant cycles allow the calculation of the free energy of interaction ($\Delta\Delta G_{int}$) between specific amino acids. A $\Delta\Delta G_{int} = 0$ is expected for completely independent mutations. The interpretation of $\Delta\Delta G_{int} \neq 0$ is model dependent, i.e., this quantity may reflect a change in solvation resulting from the mutation of one partner in an ion pair (Horovitz et al., 1990) and/or an associated conformational change (Serrano et al., 1990).

Table 3. *Donor/acceptor double mutagenesis evaluations of the free energy contributions of the hydrogen bonds in the HyHEL-10/HEWL complex*

HyHEL10	HEWL	$\Delta\Delta G^a$ kcal/mol (scFv-10 mutation)	$\Delta\Delta G^b$ kcal/mol (HEWL mutation)
V_L			
N31 Oδ1	K96 Nζ	5.2 ± 0.1 ($N31_LA$)	6.8 ± 0.1 (K96M)
N32 Nδ2	G16 O	5.1 ± 0.1 ($N32_LA$)	
Q53 Oϵ1	N93 Nδ2	1.0 ± 0.2 ($Q53_LA$)	0.6 ± 0.1 (N93A)
Q53 Nϵ2	N93 Oδ1		
S91 O	Y20 OH		−0.4 ± 0.1 (Y20F)
Y96 OH	R21 NH1	1.4 ± 0.2 ($Y96_LF$)	1.1 ± 0.1 (R21A)
V_H			
S31 Oγ	R73 NH1	0.2 ± 0.3 ($S31_HA$)	−0.3 ± 0.1 (R73A)
T30 O	R73 NH1		−0.3 ± 0.1 (R73A)
Y33 OH	K97 O	1.1 ($Y33_HF$)[c]	
Y50 OH	R21 NH1, S100 O	1.7 ($Y50_HF$)[c]	1.1 ± 0.1 (R21A)
Y53 O	D101 Oδ1		1.5 ± 0.1 (D101A)
Y58 OH	G102 N	0.4 ($Y58_HF$)[c]	

[a] $\Delta\Delta G = RT \ln(K_d[\text{mutant scFv-10 complex}]/K_d[\text{WT scFv-10 complex}])$ with wt HEWL.
[b] $\Delta\Delta G = RT \ln(K_d[\text{mutant HEWL complex}]/K_d[\text{WT HEWL complex}])$ with wt scFV-10.
[c] Values from Tsumoto et al. (1995).

Double mutant cycles for 12 amino acid pairs in the HyHEL-10/HEWL interface were constructed to understand more fully the energetic contributions obtained for the single mutants. Seven of these 12 pairs have side chains that are appropriately positioned to form H-bonds, salt bridges, or significant van der Waals contacts while the other five are well separated. The results for contacting pairs are shown in Table 2. The $\Delta\Delta G_{int}$ for any complex for which the HEWL residue probed is a major immunodeterminant, i.e., K96 or K97 (Rajpal et al., 1998), is very close to the loss of free energy observed for the HyHEL-10 single mutant, i.e., from Equation 1.

$$\Delta\Delta G_{int} = \Delta\Delta G_{A\to A'}$$

$$\therefore\ \Delta\Delta G_{B\to B'} = \Delta\Delta G_{AB\to A'B'} \qquad (2)$$

where A and B refer to the antibody and HEWL, respectively. In other words the $\Delta\Delta G$ associated with the double mutation is realized entirely by mutation of the lysozyme hot spot.

Although the $\Delta\Delta G_{int}$ values for remote pairs of amino acids are generally small (Table 4), there are two exceptions: the $Y50_LA$/K97A and the $W95_HA$/K96A pairs. One interpretation is that the $Y50_LA$ or $W95_HA$ mutations effect a conformational change that allows the recapture elsewhere in the complex of some of the free energy lost when the K97A or K96A mutation is introduced into the WT antibody complex, e.g., $7.3 < (6.2 + 4.6)$ kcal/mol, for $Y50_LA$/K97A, because less free energy of association is lost in the double mutant than in the sum of the two single mutants. This interpretation is supported by the observation that the correspondingly more conservative $Y50_LF$ and $W95_HF$ mutants do not bind as well ($\Delta\Delta G > 8.5$ kcal/mol) to the K97A and K96A HEWL as do the $Y50_LA$ and $W95_HA$ antibodies, while the opposite situation is obtained for association with WT HEWL (Table 4). The values of $\Delta\Delta G_{int}$ are small for the double mutant cycles not involving K96 or K97 (Table 4).

Mariuzza's laboratory has recently published the results of double mutant cycle analyses with the antibody D1.3/HEWL complexes (Dall'Acqua et al., 1998) and the D1.3/E5.2 (Goldman et al., 1997) complexes, E5.2 is an anti-idiotypic antibody. The values of K_D are both in the 10 nM range. These complexes are about 300-fold less stable than the HyHEL-10/HEWL complex. Comparison of the results of single and double mutations between high affinity and weaker complexes is instructive. A clear difference is the observation that no single amino acid in HEWL makes a comparable contribution to the free energy of association with

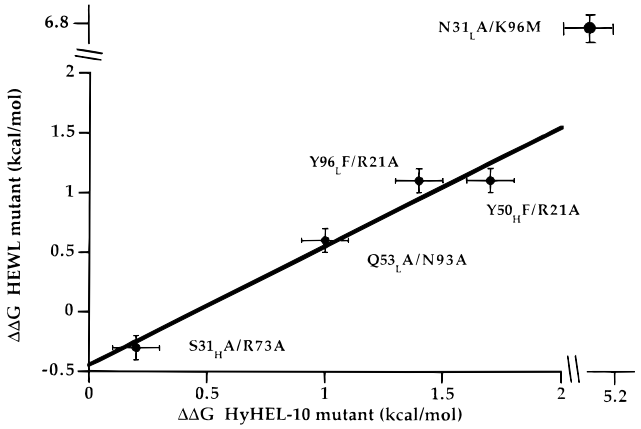

Fig. 2. Correspondence between $\Delta\Delta G$ values obtained by mutation of either H-bonding partner in the HyHEL-10/HEWL. The specific mutants are labeled. The slope of the line excluding the $N31_LA$/K96M pair is 1.0.

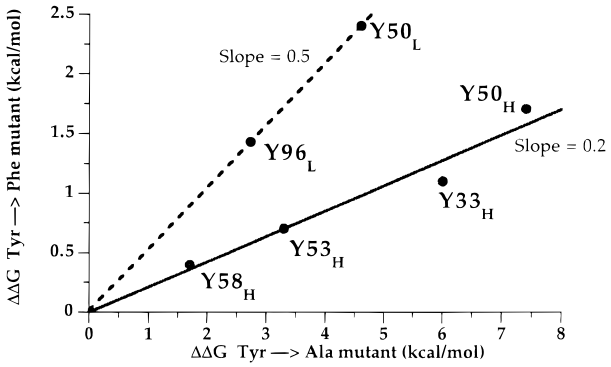

Fig. 3. Free energy changes in the HyHEL-10/HEWL complex stability for Tyr → Phe mutation plotted against the corresponding Tyr → Ala free energy changes. The dotted line is for the residues of the light chain (slope 0.5), and the solid line is for those of the heavy chain (slope 0.2).

Table 4. *Double mutant cycle analysis of the coupling energies between the indicated mutant pairs in the HyHEL-10-HEWL complex for noncontacting residues*[a]

HyHEL-10 mutants	$\Delta\Delta G$[b] (kcal/mol) HyHEL-10 mutants	HEWL mutants	$\Delta\Delta G$[b] (kcal/mol) HEWL mutants	$\Delta\Delta G$[b] (kcal/mol) Double mutant	Distance between residues[c] (Å)	$\Delta\Delta G_{int}$[d] (kcal/mol)
V_L						
$Y50_LA$	4.6 ± 0.1	Y20A	4.9 ± 0.1	NB[e]	5.6	NA[f]
$Y50_LA$	4.6 ± 0.1	R21A	1.1 ± 0.1	6.4 ± 0.2	9.5	−0.7 ± 0.2
$Y50_LA$	4.6 ± 0.1	K97A	6.2 ± 0.1	7.3 ± 0.6	5.8	3.5 ± 0.6
$Y50_LF$	2.4 ± 0.2	Y20A	4.9 ± 0.1	6.3 ± 0.1	5.6	1.0 ± 0.2
$Y50_LF$	2.4 ± 0.2	R21A	1.1 ± 0.1	4.4 ± 0.2	9.5	−0.9 ± 0.3
$Y50_LF$	2.4 ± 0.2	K97A	6.2 ± 0.1	NB	5.8	NA
V_H						
$W95_HA$	5.5 ± 0.2	Y20A	4.9 ± 0.1	NB	4.5	NA
$W95_HA$	5.5 ± 0.2	K96A	7.0 ± 0.3	7.7 ± 0.7	6.4	4.8 ± 0.8
$W95_HF$	3.2 ± 0.2	K96A	7.0 ± 0.3	NB	6.4	NA

[a] From Padlan et al. (1989).
[b] The $\Delta\Delta G$ values are defined as $\Delta\Delta G = RT \ln(K_{mut\_complex}/K_{WT\_complex})$, where K is the dissociation constant.
[c] Closest distance between side chains for the WT residues in Å (PDB file 3HFM).
[d] Coupling energies are defined in Table 2.
[e] NB, no binding was detected at 20 μM HyHEL-10; therefore $K_D > 40$ μM, $\Delta\Delta G > 8.5$ kcal/mol.
[f] Not available, see footnote e.

the D1.3 antibody as do the three previously identified dominant residues of HEWL in the HyHEL-10 complex. Alanine scanning has provided values of $\Delta\Delta G$ = 4.2, 7.0, and 6.1 for the Y20A, K96A, and K97A complexes, respectively (Rajpal et al., 1998); whereas the largest effect of an Ala replacement of HEWL in the D1.3 complex, Q121A, decreases the stability only by 2.0 kcal/mol. The same two complexes also show striking differences in alanine scanning mutagenesis of the paratope. Six of the 12 alanine substitutions in the HyHEL-10 paratope yield $\Delta\Delta G$ values ≥4 kcal/mol (Fig. 1), while only one of nine in the weaker D1.3/HyHEL-10 complex is that large.

Errors in double mutant cycle analysis

The following considerations argue that the quantitative value of double mutant cycle results is limited to analysis of large values of $\Delta\Delta G_{int}$ unless data of more than typical precision are collected. The propagated error in $\Delta\Delta G_{int}$ (Equation 1), $\sigma_{\Delta\Delta G_{int}}$ *is*

$$\sigma_{\Delta\Delta G_{int}} = \sqrt{\sigma_{\Delta\Delta G_{A\to A'}})^2 + (\sigma_{\Delta\Delta G_{B\to B'}})^2 + (\sigma_{\Delta\Delta G_{AB\to A'B'}})^2}. \quad (3)$$

Typical reported errors in the determination of values of K_D range from 12% (Schreiber & Fersht, 1995; Frisch et al., 1997; Schreiber et al., 1997) to 30% (Dall'Acqua et al., 1996, 1998; Goldman et al., 1997) or a spread between those values (Ackermann et al., 1998). Those reported here are 10–15%, except for very deleterious double mutants where they increase to 50% (Appendix). These values represent the reported precision not the accuracy. Some subsequent determinations of the identical constructs from the same laboratory using the same or an alternative technique yield significantly more variation.

Table 5 reports the calculated propagated errors in $\Delta\Delta G_{int}$ for a range of *percent* errors in the individual K_D determinations. For example, a 30% error in K_D values propagates to an error of 1 kcal/mol in $\Delta\Delta G_{int}$. Many workers consider a spread of 2σ values (90% confidence level) to be a satisfactory threshold level of quantitative significance (Schreiber et al., 1997). This means, for example, that errors in K_D values must be ≤20% to draw meaningful conclusions for $\Delta\Delta G_{int} \leq 2$ kcal/mol. This figure falls well within the range of H-bond interactions. The conclusion is that without highly precise data, double mutant cycle analysis can only be applied with confidence to the consideration of "hot spots."

Table 5. *Sensitivity of propagated error in free energy of interaction calculated from double mutant cycles to the error in the individual equilibrium constants (K_D or K_A)*

$\sigma(K_D)$ or $\sigma(K_A)$[a] (%)	$\sigma(\Delta G_A)$[b] (kcal/mol)	$\sigma(\Delta\Delta G_{A\to A'})$[c] (kcal/mol)	$\sigma(\Delta\Delta G_{int})$[d] (kcal/mol)
10	0.14	0.19	0.33
20	0.27	0.38	0.67
30	0.41	0.58	1.00
50	0.68	0.96	1.67
100	1.36	1.92	3.33

[a] Percent errors in the individual determination of K_D values.
[b] $2.303RT(\sigma(K_D)/K_D)$.
[c] Propagated error for $\Delta G_A - \Delta G_{A'}$: $\sqrt{\sigma(\Delta G_A)^2 + \sigma(G_{A'})^2}$.
[d] Equation 3.

Material and methods

The materials and procedures not described here are to be found in Rajpal et al. (1998).

HyHEL-10 expression and purification

All determinations were carried out with the scFv gene for the monoclonal antibody HyHEL-10 (scFv-10), a gift of Professor Andreas Plückthun. The scFv-10 gene was cloned with *Xho*I/*Avr*II into the pPIC-9 secretion vector for *Pichia pastoris* (Invitrogen, Carlsbad, California). Five histidine residues were added to the C-terminus to allow Ni-column purification. The recombinant plasmid was linearized by *Stu*I restriction digest for genomic integration into *P. pastoris* GS115. Transformants were selected for their capacity to grow in histidine free media. One of 10 transformants showing the highest expression level was used to express the protein in BMMY media (1% yeast extract, 2% peptone, 1.34% yeast nitrogen base, 0.5% methanol, 4×10^{-5}% biotin, 100 mM potassium phosphate, pH 6.0). Expression cultures were incubated at 30 °C for 5 days inducing with 0.5% methanol (final concentration) every 12 h. The culture was centrifuged (11,000 *g*, 15 min), the supernatant collected, the pH adjusted to 7.0 with KOH, and the suspension centrifuged (11,000 *g*, 30 min) to remove precipitated proteins. The supernatant was loaded onto Ni-NTA (nitrolotriacetic acid) superflow resin (Qiagen, Hilden, Germany) equilibrated with 66 mM potassium phosphate buffer, pH 7.0, 300 mM KCl. The column was washed with 5 volumes of 66 mM potassium phosphate buffer, pH 7.0, 300 mM KCl, and the scFv-10 was eluted with a shallow linear gradient of imidazole (0–0.3 M in the same buffer). Fractions enriched (analyzed by SDS-PAGE) with scFv-10 were pooled and dialyzed against 66 mM potassium phosphate buffer, pH 7.0. The purity of the samples was verified by SDS-PAGE. Absence of glycosidation was confirmed by mass spectrometry and no dimers were detected by HPLC gel filtration (Bio-sil-sec 250 Column, Bio-Rad, Richmond, California). The proteins were stored at low concentration to minimize dimerization (<0.5 mg/mL, Dougan et al., 1998). Mutant proteins were concentrated by Centriprep-10 prior to use when required. The concentration of scFv-10 was determined with the molar extinction coefficient ($\epsilon_{280} = 53{,}200\ M^{-1}\ cm^{-1}$, calculated from the amino acid sequence and verified for the WT protein by titration with HEWL). Twenty to 50 mg of purified protein per liter of culture were typically obtained.

Site-directed mutagenesis

The HEWL mutant genes were available from previous investigations of this laboratory (Rajpal et al., 1998; Taylor et al., 1998). The HyHEL-10 mutants were produced by PCR with the megaprimer method (Landt et al., 1990; Pons et al., 1997). All mutants were fully sequenced.

Determination of kinetic parameters for complex formation and dissociation

HyHEL-10 occludes the active site of HEWL. The complex has only 5% of the catalytic activity of free HEWL; therefore, the extent of HyHEL-10 association with HEWL can be determined in homogeneous solution by monitoring the rate of loss of activity of HEWL following addition of HyHEL-10 as described by Taylor et al. (1998). The values of k_{on} were determined from nonlinear regression of the data from Equation 4.

$$Abs_{obs} = Abs_{init} + v_{bl} \cdot t - \left[\frac{k_{cat} \cdot [E_T] \cdot [S]}{k_{on} \cdot K_m \cdot [Ab_T]} \cdot \left(1 - e^{\frac{k_{on} \cdot [Ab_T] \cdot K_m \cdot t}{K_m + [S]}} \right) \right] \quad (4)$$

where Abs_{init} = initial absorbance at 450 nm, v_{bl} = settling rate of the substrate cell wall particles in the absence of HEWL, $[E_T]$ = total concentration of HEWL, $[Ab_T]$ = total scFv-10 concentration, and $[S]$ = initial substrate *Micrococcus luteus* cell wall concentration. Only those fits to Equation 4 yielding a correlation coefficient R of ≥0.995 were accepted.

The dissociation rate constants k_{off} were determined by monitoring the rate of recovery of active HEWL from a preformed HyHEL-10/HEWL complex. The nascent free antibody was sequestered with an excess of E35Q HEWL, an inactive mutant. The data were fitted to Equation 5 (Rajpal et al., 1998).

$$v_{obs} = k_{cat} \cdot [E_T] \cdot (1 - e^{-k_{off} \cdot t}) + v_{init} \cdot (e^{-k_{off} \cdot t}) + v_{bl} \quad (5)$$

where v_{init} = enzymatic activity due to the complex and trace amounts of HEWL before the addition of E35Q HEWL. The kinetic assays were performed at pH 7.0 instead of pH 6.2 to eliminate scFv-10 precipitation (pI = 6.0, calculated from the amino acid composition). The k_{on} and k_{off} values for the formation and dissociation of the scFv-10/HEWL(WT) complex at pH 7.0 were similar to those obtained at pH 6.2 (data not shown). All data were obtained on a Uvikon 860 (Kontron Instruments, San Diego, California) spectrophotometer and fitted by nonlinear regression to their respective models utilizing the application Kaleidagraph (Synergy Software, Reading, Pennsylvania).

When K_D values are greater than 3 nM (100 × K_D WT), the kinetics are too fast to monitor by these methods; in these cases, only the values of K_D determined by equilibrium methods (Kam-Morgan et al., 1993) are given. All scFv-10 concentrations were <20 μM.

Appendix. *Experimental data set*

Complex (scFV-HEL)	k_{on} ($10^6\ M^{-1}\ s^{-1}$)	err k_{on} ($10^6\ M^{-1}\ s^{-1}$)	k_{off} (10^{-4} 1/s)	err k_{off} (10^{-4} 1/s)	K_D (nM)	err K_D (nM)	$\Delta\Delta G$ (kcal/mol)	err $\Delta\Delta G$ (kcal/mol)
wt-wt	1.88	0.08	0.54	0.002	0.03	0.001	—	—
Interaction HEL Y20								
wt-Y20A					113	8	4.9	0.11
$N32_LA$-wt					167	27	5.13	0.22
$N32_LA$-Y20A						NO binding at 4 μM scFv		

(*continued*)

Appendix. *Continued*

Complex (scFV-HEL)	k_{on} (10^6 M^{-1} s^{-1})	err k_{on} (10^6 M^{-1} s^{-1})	k_{off} (10^{-4} 1/s)	err k_{off} (10^{-4} 1/s)	K_D (nM)	err K_D (nM)	$\Delta\Delta G$ (kcal/mol)	err $\Delta\Delta G$ (kcal/mol)
Interaction HEL K96								
wt-K96A					4,000	800	7.00	0.27
$N31_LA$-wt					200	20	5.20	0.15
$N31_LA$-K96A					9,000	2,000	7.5	0.30
$N31_LD$-wt	1.26	0.07	3.68	0.7	0.29	0.06	1.4	0.28
$N31_LE$-wt					460	40	5.7	0.13
$Y50_LA$-wt					66	6	4.6	0.13
$Y50_LL$-wt					50	4	4.4	0.12
$Y50_LF$-wt	1.25	0.02	20.6	2.5	1.6	0.2	2.4	0.18
$Y50_LA$-R21A					1,400	200	6.4	0.19
$Y50_LF$-R21A					45	6	4.36	0.19
$Y50_LF$-Y20A					1,100	100	6.3	0.13
$Y50_LA$-K96A					14,000	11,000	7.8	1.06
$Y50_LA$-K97A					7,000	3,000	7.30	0.58
$Y50_LF$-K97A						NO binding at 20 μM scFv		
$Y50_LF$-K96A						NO binding at 20 μM scFv		
$Y50_LA$-Y20A						NO binding at 8 μM scFv		
Interaction HEL K97								
wt-K97A					1,000	50	6.2	0.08
$Y33_HA$-wt					800	80	6.0	0.15
$Y33_HA$-K97A					6,000	1,000	7.2	0.23
$Y33_HA$-K96A						NO binding at 10 μM scFv		
$Y33_HA$-Y20A						NO binding at 10 μM scFv		
[a]$Y33_HF$-wt							1.1	
$W95_HF$-K97A						NO binding at 20 μM scFv		
$W95_HF$-wt					7.2	0.8	3.27	0.16
$W95_HF$-Y20A					1,110	80	6.26	0.11
$W95_HA$-wt					330	40	5.5	0.17
$W95_HA$-K97A						No binding at 10 μM scFv		
$W95_HA$-K96A					14,000	7,000	7.7	0.68
$W95_HF$-K96A						No binding at 10 μM scFv		
$W95_HA$-Y20A						LOW binding at 8 μM scFv		
$D32_HA$-wt	1.6	0.1	11.90	0.1	0.74	0.03	1.93	0.07
$D32_HA$-K97A					70	10	4.62	0.19
$D32_HN$-K97A					116	7	4.92	0.09
$D32_HN$-wt	2.01	0.04	0.33	0.1	0.04	0.01	0.2	0.3
$D32_HA$-K97M	2.9	0.1	5.8	0.3	0.2	0.01	1.14	0.08
$D32_HN$-K97M	2.46	0.1	1.12	0.01	0.05	0.002	0.27	0.07
wt-K97M	1.53	0.05	2.8	0.1	0.19	0.01	1.1	0.08
Noninteracting with HEL hot spots								
wt-R21A	1.56	0.06	2.71	0.16	0.17	0.01	1.07	0.09
$S31_HA$-wt	1.24	0.06	0.48	0.08	0.04	0.01	0.18	0.34
$Y50_HA$-wt					7,000	2,000	7.4	0.39
[a]$Y50_HF$-wt							1.7	
$Y50_HA$-R21A					20,000	10,000	8.0	0.68
$Q53_LA$-wt	1.37	0.05	2.0	0.2	0.15	0.02	0.96	0.18
$Y96_LA$-wt	0.8	0.03	23.00	0.06	2.9	0.11	2.73	0.07
$Y96_LA$-R21A					500	100	5.7	0.27
$Y96_LF$-R21A					35	5	4.21	0.19
$Y96_LF$-wt	1.4	0.1	4.5	0.3	0.32	0.04	1.43	0.18
[a]$Y53_HA$-wt							3.3	
[a]$Y53_HF$-wt							0.7	
[a]$Y58_HA$-wt							1.7	
[a]$Y58_HF$-wt							0.4	

[a]From Tsumoto et al. (1995).

Acknowledgments

We wish to thank Professor Andreas Plückthun for the generous gift of the gene for the scFv form of HyHEL-10. We are additionally grateful to Ms. Tinh Luong for help with the analysis of the X-ray structure and Dr. Douglas Burdette for initial work on scFv expression in *P. pastoris*. This work was supported by the Director, Office of Energy Research, Office of Basic Energy Sciences, Divisions of Material Sciences and of Energy Biosciences of the U.S. Department of Energy under Contract No. DE-AC03-76SF00098 to Lawrence Berkeley National Laboratory. Jaume Pons was supported by a postdoctoral fellowship from Ministerio de Educación y Cultura (Spain).

References

Ackermann EJ, Ang ET, Kanter JR, Tsigelny I, Taylor P. 1998. Identification of pairwise interactions in the alpha-neurotoxin-nicotinic acetylcholine receptor complex through double mutant cycles. *J Biol Chem 273*:10958–10964.

Alber T, Dao-Pin S, Nye JA, Muchmore DC, Matthews BW. 1987. Temperature-sensitive mutations of bacteriophage T4 lysozyme occur at sites with low mobility and low solvent accessibility in the folded protein. *Biochemistry 26*:3754–3758.

Carter PJ, Winter G, Wilkinson AJ, Fersht AR. 1984. The use of double mutants to detect structural changes in the active site of the tyrosyl-tRNA synthetase (*Bacillus stearothermophilus*). *Cell 38*:835–840.

Chothia C, Lesk AM, Tramontano A, Levitt M, Smith-Gill SJ, Air G, Sheriff S, Padlan EA, Davies D, Tulip WR, Colman PM, Spinelli S, Alzari PM, Poljak RJ. 1989. Conformations of immunoglobulin hypervariable regions. *Nature 342*:877–883.

Clackson T, Ultsch MH, Wells JA, de Vos AM. 1998. Structural and functional analysis of the 1:1 growth hormone: Receptor complex reveals the molecular basis for receptor affinity. *J Mol Biol 277*:1111–1128.

Clackson T, Wells JA. 1995. A hot spot of binding energy in a hormone-receptor interface. *Science 267*:383–386.

Dall'Acqua W, Goldman ER, Eisenstein E, Mariuzza RA. 1996. A mutational analysis of the binding of two different proteins to the same antibody. *Biochemistry 35*:9667–9676.

Dall'Acqua W, Goldman ER, Wenhong L, Teng C, Tsuchiya D, Li H, Ysern X, Braden BC, Li Y, Smith-Gill SJ, Mariuzza RA. 1998. A mutational analysis of binding interactions in an antigen-antibody protein-protein complex. *Biochemistry 37*:7981–7991.

Davies DR, Cohen GH. 1996. Interactions of protein antigens with antibodies. *Proc Natl Acad Sci USA 93*:7–12.

Dougan DA, Malby RL, Gruen LC, Kortt AA, Hudson PJ. 1998. Effects of substitutions in the binding surface of an antibody on antigen affinity. *Protein Eng 11*:65–74.

Fersht AR, Shi J, Knill-Jones J, Lowe DM, Wilkinson AJ, Blow DM, Brick P, Carter P, Waye MM, Winter G. 1985. Hydrogen bonding and biological specificity analyzed by protein engineering. *Nature 314*:235–238.

Frisch C, Schreiber G, Johnson CM, Fersht AR. 1997. Thermodynamics of the interaction of barnase and barstar: Changes in free energy versus changes in enthalpy on mutation. *J Mol Biol 267*:696–706.

Goldman ER, Dall'Acqua W, Braden BC, Mariuzza RA. 1997. Analysis of binding interactions in an idiotope-antiidiotope protein-protein complex by double mutant cycles. *Biochemistry 36*:49–56.

Goodman HM, Frick GP, Souza S. 1996. Species specificity of the primate growth hormone receptor. *News Physiol Sci 11*:157–161.

Hendsch ZS, Tidor B. 1994. Do salt bridges stabilize proteins? A continuum electrostatic analysis. *Protein Sci 3*:221–226.

Horovitz A, Serrano L, Avron B, Bycroft M, Fersht AR. 1990. Strength and cooperativity of contributions of surface salt bridges to protein stability. *J Mol Biol 216*:1031–1044.

Janin J, Chothia C. 1990. The structure of protein-protein recognition sites. *J Biol Chem 265*:16027–16030.

Kabat EA, Wu TT, Bilofsky H. 1977. Unusual distribution of amino acids in complementarity-determining (hypervariable) segments of heavy and light chains of immunoglobulins and their possible roles in specificity of antibody combining sites. *J Biol Chem 252*:6609–6616.

Kabat EA, Wu TT, Perry HM, Gottesman KS, Foeller C. 1991. Sequences of proteins of immunological interest. NIH Publication 91-3242. Bethesda, MD: National Institutes of Health.

Kam-Morgan LNW, Smith-Gill SJ, Taylor MG, Zhang L, Wilson AC, Kirsch JF. 1993. High-resolution mapping of the HyHEL-10 epitope of chicken lysozyme by site-directed mutagenesis. *Proc Natl Acad Sci USA 90*:3958–3962.

Landt O, Grunert HP, Hahn U. 1990. A general method for rapid site-directed mutagenesis using the polymerase chain reaction. *Gene 96*:125–128.

Manning TC, Schlueter CJ, Brodnicki TC, Parke EA, Speir JA, Garcia C, Teyton L, Wilson IA, Kranz DM. 1998. Alanine scanning mutagenesis of an $\alpha\beta$ T crell receptor: Mapping the energy of antigen recognition. *Immunity 8*:413–425.

Martin ACR, Thornton JM. 1996. Structural families in loops of homologous proteins: Automatic classification, modeling and application to antibodies. *J Mol Biol 263*:800–815.

Mian S, Bradwell AR, Olson AJ. 1991. Structure, function and properties of antibody binding sites. *J Mol Biol 217*:133–151.

Padlan EA. 1990. On the nature of antibody combining sites: Unusual structural features that may confer on these sites an enhanced capacity for binding ligands. *Proteins Struct Funct Genet 7*:112–124.

Padlan EA, Silverton EW, Sheriff S, Cohen GH, Smith-Gill SJ, Davies DR. 1989. Structure of an antibody-antigen complex: Crystal structure of the HyHEL-10 Fab-lysozyme complex. *Proc Natl Acad Sci USA 86*:5938–5942.

Pomès R, Willson RC, McCammon JA. 1995. Free energy simulations of the HyHEL-10/HEL antibody-antigen complex. *Protein Eng 8*:663–675.

Pons J, Planas A, Juncosa M, Querol E. 1997. PCR site-directed mutagenesis using *Pyrococcus sp* GB-D polymerase coupled to a rapid screening procedure. In: White BA, ed. *PCR cloning protocols, Vol. 67*. New York: Humana Press. pp 209–218.

Pons J, Planas A, Querol E. 1995. Contribution of a disulfide bridge to the stability of 1,3-1,4-β-D-glucan 4-glucanhydrolase from *Bacillus licheniformis*. *Protein Eng 8*:938–945.

Rajpal A, Taylor MG, Kirsch JF. 1998. Quantitative evaluation of the chicken lysozyme epitope in the HyHEL-10 Fab complex: Free energies and kinetics. *Protein Sci 7*:1868–1874.

Schreiber G, Fersht AR. 1995. Energetics of protein-protein interactions: Analysis of the barnase-barstar interface by single mutations and double mutant cycles. *J Mol Biol 248*:478–486.

Schreiber G, Frisch C, Fersht AR. 1997. The role of Glu73 of barnase in catalysis and binding of barstar. *J Mol Biol 270*:111–122.

Serrano L, Horovitz A, Avron B, Bycroft M, Fersht AR. 1990. Estimating the contribution of engineered surface electrostatic interactions to protein stability by using double-mutant cycles. *Biochemistry 29*:9343–9352.

Serrano L, Kellis JTJ, Cann P, Matouschek A, Fersht AR. 1992. The folding of an enzyme—II. Substructure of barnase and the contribution of different interactions to protein stability. *J Mol Biol 224*:783–804.

Smith-Gill SJ, Lavoie TB, Mainhart CR. 1984. Antigenic regions defined by monoclonal antibodies correspond to structural domains of avian lysozyme. *J Immunol 133*:384–392.

Souza SC, Frick GP, Wang X, Kopchick JJ, Lobo RB, Goodman HM. 1995. A single arginine residue determines species specificity of the human growth hormone receptor. *Proc Natl Acad Sci USA 92*:959–963.

Taylor MG, Rajpal A, Kirsch JF. 1998. Kinetic epitope mapping of the chicken lysozyme/HyHEL-10 Fab complex: Delineation of docking trajectories. *Protein Sci* 7:1857–1867

Tsumoto K, Ogasahara K, Ueda Y, Watanabe K, Yutani K, Kumagai I. 1995. Role of Tyr residues in the contact region of anti-lysozyme monoclonal antibody HyHEL-10 for antigen binding. *J Biol Chem 270*:18551–18557.

Tsumoto K, Ogasahara K, Ueda Y, Watanabe K, Yutani K, Kumagai I. 1996. Role of salt bridge formation in antigen-antibody interaction. *J Mol Biol 271*:32612–32616.

Wells JA. 1996. Binding in the growth hormone receptor complex. *Proc Natl Acad Sci USA 93*:1–6.

Xavier KA, Willson RC. 1998. Association and dissociation kinetics of anti-hen egg lysozyme monoclonal antibodies HyHEL-5 and HyHEL-10. *Biophys J 74*:2036–2045.

Ysern X, Li H, Mariuzza RA. 1998. Imperfect interfaces [news]. *Nature Struct Biol 5*:412–414.